CLOSED FORM CALIBRATION OF 1BIT/2LEVEL CORRELATOR USED FOR SYNTHETIC APERTURE INTERFEROMETRIC RADIOMETER

Cheng Zheng[*], Xianxun Yao, Anyong Hu, and Jungang Miao

School of Electronic and Information Engineering, Beihang University, Xueyuan Road 37th, Haidian District, Beijing 100191, China

Abstract—A Ka-band two-dimensional synthetic aperture interferometric radiometer called BHU-2D has been developed by Electromagnetic Engineering Laboratory of Beihang University. The radiometer obtains images in real-time benefiting from the adoption of a 1bit/2level FPGA-based correlator unit. The design and implementation of the correlator unit in BHU-2D are presented in this paper. The calibration procedures of the correlation coefficients are also presented. For the purpose of simplifying the calibration procedure, a closed form approximation is introduced and applied to BHU-2D, which is used to correct the errors caused by threshold offset of the quantizer. Error analysis of this approximation shows that the method is applicable in SAIRs. In order to verify the design and calibration method, a series of validation experiments have been conducted. Measurement results have proved that the performance of the correlation unit could meet the requirements of BHU-2D.

1. INTRODUCTION

Synthetic aperture interferometric radiometer (SAIR) was introduced in the late 1980s as an alternative to real aperture radiometers for earth observation [1]. Through interferometry by an array of small antennas, SAIR realizes large equivalent aperture, and in turn achieves high resolution at low microwave frequencies with reduced mass and mechanical requirements. A SAIR is a group of interferometers. The interferometers measure the complex cross correlations between signals received by each pair of antennas. Each complex correlation

measured by the SAIR can be called a sample of the visibility function. Based on Van-Cittert-Zernike Theorem [2], visibility function could be approximated by the spatial Fourier transform of the brightness temperature within the field of view (FOV).

A new SAIR called BHU-2D has been developed by Beihang University since 2006 [3]. The instrument operates at $34.02 \sim 34.18$ GHz and consists of 24 receiving elements. Therefore, $276(= 24 \times 23/2)$ complex cross-correlations can be measured. To computes the 276 complex cross-correlations, a digital correlator unit is designed. The digital correlator unit includes a group of analogue-to-digital converters (ADC) and a data processing component. Considering the complex bandwidth of the baseband signal is 160 MHz, 200 MHz is selected as the sampling rate of the correlator unit, which meets the Nyquist Theorem in complex frequency domain and makes full use of the receiving bandwidth. In order to compute all the 276 complex cross-correlations simultaneously with a working frequency of 200 MHz and obtain brightness temperature images in real-time, a FPGA is used to form the processing component. To reduce the complexity and power consumption of the correlator unit, 1bit/2level (1B/2L) correlator is employed in BHU-2D.

The design of the correlator unit in BHU-2D is presented in this paper. Firstly, the principle of the 1B/2L correlator is reviewed and the calibration methods of the correlation coefficients are introduced in Section 2. In order to simplify the calibration procedure, a new closed form approximation to correct threshold offset errors is employed. The error caused by the approximation is also discussed in Section 2. And then, the configuration of the correlator unit in BHU-2D is described in Section 3. To verify the design of the correlator unit, experiments are conducted and the results are shown in Section 4. The results proved that the performance of the correlator unit could meet the requirements of BHU-2D.

2. DESIGN

2.1. Principle

The main idea of 1B/2L correlator is to calculate the correlation between signals which are digitized into just 1-bit rather than multi-bit. Being digitized into 1-bit, the signal fed into the correlator can be expressed as

$$x_n = g[x(nT)] = \begin{cases} 1 & x(nT) \geq 0 \\ -1 & x(nT) < 0 \end{cases} \qquad n = 0, 1, 2, \ldots \qquad (1)$$

where $x(t)$ is the input signal, T the sampling period, and $g[\cdot]$ the quantization function. The 1B/2L correlation between signals $x(t)$ and $y(t)$ can be expressed as

$$\mu_2 = E\left[x_n y_n\right] = E\left\{g\left[x(nT)\right]g\left[y(nT)\right]\right\} \tag{2}$$

where $E\left[\cdot\right]$ is mathematical expectation. Because the signals measured by a radiometer are spontaneous electromagnetic radiation of the object, the input signals of the correlator for a given target could be formulated as two stationary, ergodic, zero mean Gaussian random processes and the joint probability density function (PDF) is formulated by

$$p(x,y) = \frac{1}{2\pi\sigma^2\sqrt{1-\mu^2}}\exp\left\{-\frac{x^2+y^2-2xy\mu}{2\sigma^2\left(1-\mu^2\right)}\right\} \tag{3}$$

where σ are the standard deviations of the signals, and μ is the correlation coefficient. Then the joint probability density of the quantized signals is

$$p\left(x_n, y_n\right) = \frac{1}{4} + \frac{1}{2\pi}x_n y_n \arcsin\mu \tag{4}$$

Therefore, the 1B/2L correlation can be expressed as

$$\mu_2 = 1\cdot Z + (-1)\cdot(1-Z) = 2Z-1 = \frac{2}{\pi}\arcsin\mu \tag{5}$$

where $Z = P\{x_n y_n = 1\}$ is the probability that $x_n = y_n = \pm 1$. Equation (5), known as Van Vleck relationship [4], shows that 1B/2L correlator only gives the correlation coefficient of the input signals. This result could be expected because the power information is lost during the 2-level quantization process. In order to calculate the visibility function samples of the SAIR, correlation coefficient need to be denormalized

$$V = T_{sys}\mu \tag{6}$$

where T_{sys} is the system noise temperature of the receiver. T_{sys} could be obtained by measuring the output power of the receiver, since the gain of the receiver could be calibrated in a radiometer. Thus a group of power measuring units are required in SAIRs when 1B/2L correlator is employed, such as MIRAS, HUT, etc. [5, 6].

Practically, the 1 bit digitizer is implemented by a comparator and the quantization function could be expressed as

$$x_n^{\mathrm{raw}} = g^{\mathrm{raw}}[x(nT)] = \left\{\begin{array}{ll} 1 & x(nT) \geq 0 \\ 0 & x(nT) < 0 \end{array}\right. \quad n = 0,1,2,\ldots \tag{7}$$

Then Equation (2) can be converted into

$$\mu_2^{\mathrm{raw}} = 2Z^{\mathrm{raw}} - 1 \tag{8}$$

where $Z^{\text{raw}} = P\{x_n^{\text{raw}} = y_n^{\text{raw}}\}$ is the probability that $x_n^{\text{raw}} = y_n^{\text{raw}}$. Z^{raw} can be measured by a NOT-XOR gate and a counter for a given total sample number. Since NOT-XOR gate is simpler than multi-bit multiplier and could achieve higher processing speed, 1B/2L correlator is widely used in two-dimensional SAIRs, although it requires additional power measuring units and features lower signal-to-noise ratio (SNR) [5–9].

2.2. Calibration

When 1B/2L correlator is adopted, errors will be introduced by the imperfections of the digitizer. The imperfections come mainly from two sources: timing errors of the sampling clock and threshold offset of the comparator.

The timing errors of the sampling clock are discussed firstly. Timing errors include clock skew and jitter. Ignoring the slight influence on the fringe washing function, timing errors could be equivalent to the phase errors of the receivers, including in-phase and quadrature errors [10]. Actually, sampling devices can be thought as a multiplier, and the timing errors can be seemed as phase errors of the sampling clock. Therefore, timing errors could be seemed as part of the phase errors in the receivers or local oscillators. In a SAIR, in-phase errors could be calibrated by noise injection method, while quadrature errors could be calibrated by computing the cross-correlations between the in-phase and quadrature signals of the receiver [11, 12].

Another error is threshold offset, which comes from the imperfection of the comparator. Assume Δx to be the threshold offset of the comparator, the quantization function could be expressed as

$$x_{ne} = g_e[x(nT), \Delta x] = \begin{cases} 1 & x(nT) \geq \Delta x \\ -1 & x(nT) < \Delta x \end{cases} \quad n = 0, 1, 2, \ldots \quad (9)$$

According to Price Theorem [13], μ_2^{raw} suffered from the offset error could be calculated through the integration of

$$\begin{aligned}
\frac{\partial \mu_2^{\text{raw}}}{\partial \mu} &= \sigma^2 E\left[\frac{\partial g_e(x, \Delta x)}{\partial x} \cdot \frac{\partial g_e(y, \Delta y)}{\partial y}\right] \\
&= 4\sigma^2 E\left[\delta(x - \Delta x)\delta(y - \Delta y)\right] \\
&= \frac{2}{\pi\sqrt{1-\mu^2}} \exp\left[-\frac{\Delta x^2 + \Delta y^2 - 2\Delta x \Delta y \mu}{2\sigma^2(1-\mu^2)}\right] \quad (10)
\end{aligned}$$

where Δx and Δy are the offset errors of the comparators, and nT is omitted. Integration of Equation (10) does not have a closed form. However, when $|\Delta x| \ll \sigma$ and $|\Delta y| \ll \sigma$, the exponential function

could be developed into Taylor series and then

$$\mu_2^{\text{raw}} = \int_0^{\mu} \frac{\partial \mu_2^{\text{raw}}}{\partial \mu} d\mu + \mu_{20}^{\text{raw}}$$

$$\approx \frac{2}{\pi} \left[\arcsin \mu + \frac{2\Delta x \Delta y - \left(\Delta x^2 + \Delta y^2 \right) \mu}{2\sigma^2 \sqrt{1-\mu^2}} - \frac{\Delta x \Delta y}{\sigma^2} \right] + x_e y_e \qquad (11)$$

where μ_{20}^{raw} is μ_2^{raw} when $\mu = 0$ and

$$x_e = \text{erf}\left(\frac{\Delta x}{\sqrt{2}\sigma} \right) = 1 - 2E\left[g_e\left(x, \Delta x \right) \right] \qquad (12a)$$

$$y_e = \text{erf}\left(\frac{\Delta y}{\sqrt{2}\sigma} \right) = 1 - 2E[g_e(y, \Delta y)] \qquad (12b)$$

where $\text{erf}(x) = \frac{2}{\sqrt{\pi}} \int_0^x \exp\left\{ -t^2 \right\} dt$ is error function. For $|\Delta x| \ll \sigma$ and $|\Delta y| \ll \sigma$, x_e and y_e could be approximated by

$$x_e \approx \frac{\sqrt{2}\Delta x}{\sqrt{\pi}\sigma} \qquad (13a)$$

$$y_e \approx \frac{\sqrt{2}\Delta y}{\sqrt{\pi}\sigma} \qquad (13b)$$

Substituting Equation (8) into Equation (11),

$$Z^{\text{raw}} = \frac{1}{\pi} \arcsin \mu + \frac{1}{2} - \frac{1}{4\sqrt{1-\mu^2}} \left(\mu x_e^2 + \mu y_e^2 - 2x_e y_e \right) \qquad (14)$$

Considering $E[g_e(x, \Delta x)]$ can be measured by a statistic way, Equation (14) uses an iteration method for calibrating the offset error [11]. However, solving Equation (14) is of low efficiency and takes more than 80% of the processing time in digital signal processor of BHU-2D. In order to obtain a closed form approximation of μ, Equation (14) could be converted into

$$\sin\left[\pi \left(Z^{\text{raw}} - \frac{1}{2} \right) \right] = \sin\left[\arcsin \mu - \frac{\pi}{4\sqrt{1-\mu^2}} \left(\mu x_e^2 + \mu y_e^2 - 2x_e y_e \right) \right]$$

$$= \mu \cos\left[\frac{\pi}{4\sqrt{1-\mu^2}} \left(\mu x_e^2 + \mu y_e^2 - 2x_e y_e \right) \right]$$

$$- \sqrt{1-\mu^2} \sin\left[\frac{\pi}{4\sqrt{1-\mu^2}} \left(\mu x_e^2 + \mu y_e^2 - 2x_e y_e \right) \right] \qquad (15)$$

Noting that $x_e \ll 1$, $y_e \ll 1$ and $\mu < 1$, Equation (15) could be developed into Taylor series, and the estimation of μ could be

approximated by

$$\mu_e = \frac{4\cos\left(\pi Z^{\mathrm{raw}}\right) + 2\pi x_e y_e}{\pi x_e^2 + \pi y_e^2 - 4} \qquad (16)$$

Equation (16) gives a closed form approximation for calibrating errors caused by threshold offsets. The error of the method is

$$\Delta\mu(\Delta x, \Delta y, \mu) = \mu_e - \mu \qquad (17)$$

Substituting Equations (2), (8), (9), (12) into Equation (17), the symmetry relation of $\Delta\mu$ is as follows

$$\Delta\mu(\Delta x, \Delta y, \mu) = \Delta\mu(\Delta y, \Delta x, \mu) \qquad (18a)$$

$$\Delta\mu(\Delta x, \Delta y, \mu) = \Delta\mu(-\Delta x, -\Delta y, \mu) \qquad (18b)$$

$$\Delta\mu(\Delta x, \Delta y, \mu) = -\Delta\mu(\Delta x, -\Delta y, -\mu) \qquad (18c)$$

According to Equation (18), evaluation of $\Delta\mu$ could be performed within $\mu \geq 0$ and $y \geq 0$. In order to evaluate Equation (16), a logarithmic form of $\Delta\mu$ is defined as

$$\varepsilon = 10\log_{10}|\Delta\mu\left(\Delta x, \Delta y, \mu\right)| \qquad (19)$$

Fig. 1 shows the relationship between ε and threshold offsets for $\mu = 0.5$, 0.05, 0.005 and 0.0005, respectively. As could be seen, the maxim error appears on the condition of $\Delta y = \Delta x = b$ or $\Delta y = -\Delta x = b$ when b is given as the boundary of the threshold offset, i.e., $|\Delta x| \leq b$ and $|\Delta y| \leq b$. Thus, discussion below will focus on the condition of $\Delta y = |\Delta x| = b$, which is the worst case. Fig. 2 shows the errors of the correlation coefficient caused by the threshold offsets when $\Delta y = |\Delta x|$. As could be seen in Fig. 2(a), the error of the correlation coefficient without calibration is much larger than the one in Fig. 2(b), which is calibrated by the closed form approximation. Compared with the iteration method, closed form method is of higher efficiency but lower accuracy, which could be seen in Figs. 2(b) and (c).

Actually, there are usually tens of receiving channels in a SAIR system. The threshold offsets corresponding to the channels are different from each other and drifting slowly. Then the synthesized errors caused by the threshold offsets are random errors and therefore part of the radiometric uncertainty. By analyzing the required radiometric sensitivity, b could be determined. In order to simplify the analyzing, the following criterion is applied to BHU-2D:

$$|\Delta\mu| \ll \sigma_\mu \qquad (20)$$

where σ_μ is the measuring uncertainty of the correlation coefficient. The criterion makes $\Delta\mu$ negligible. The measuring uncertainty could be calculated by [14]

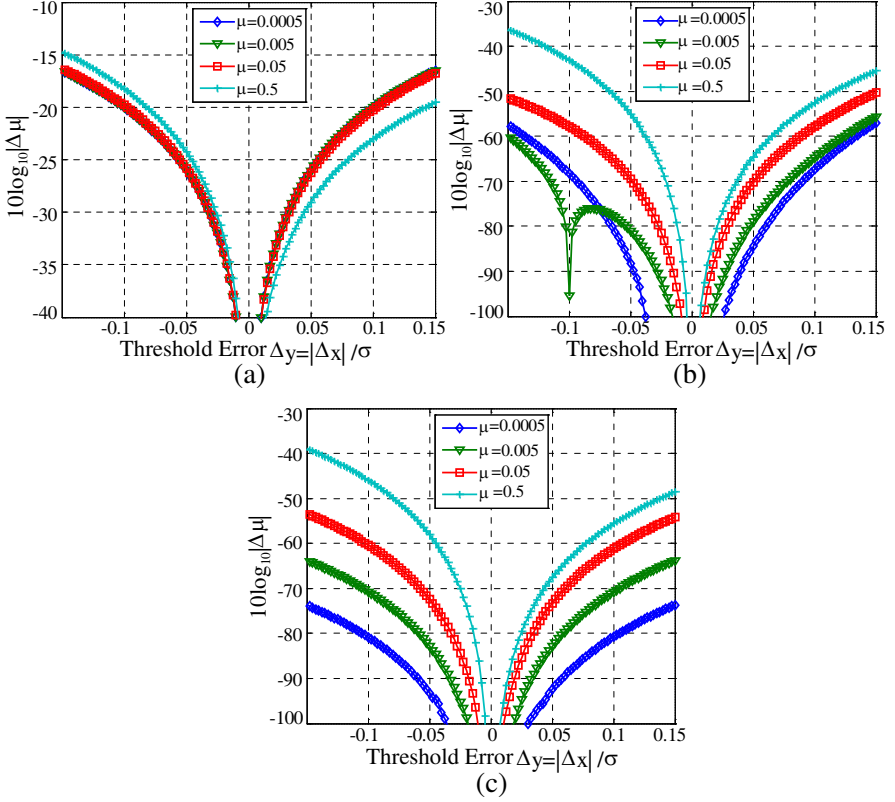$$\sigma_\mu = \frac{1}{\eta_Q\sqrt{2B\tau}} \qquad (21)$$
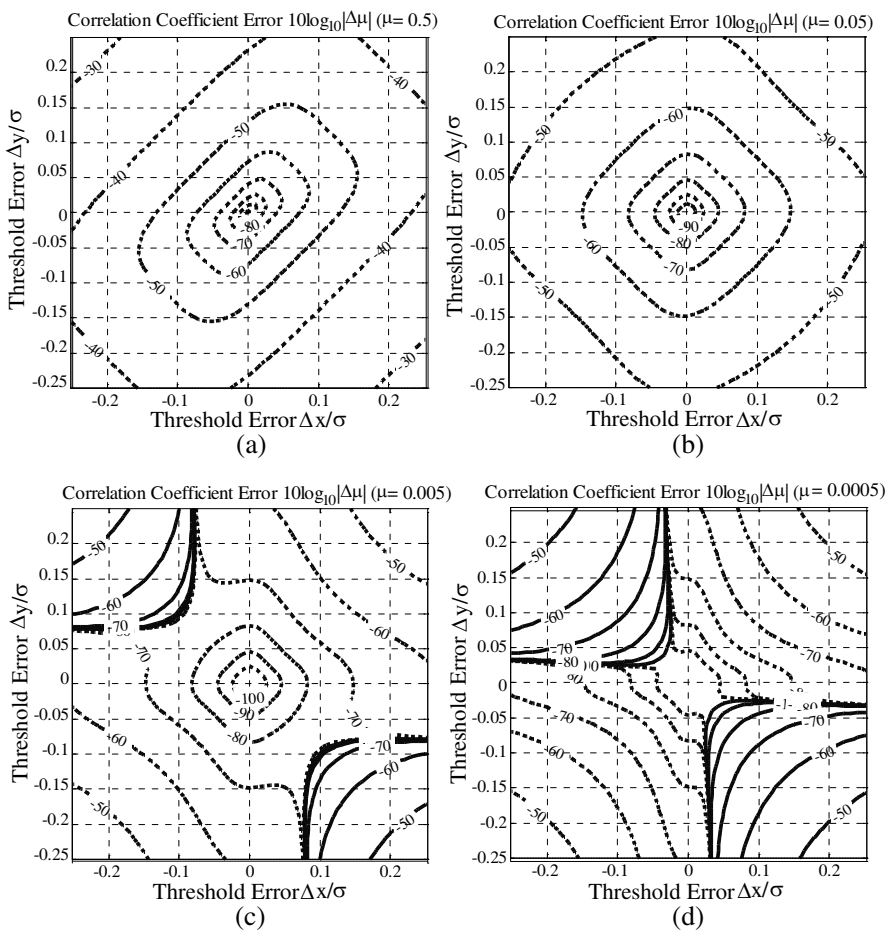
Figure 1. The relationship between correlation error and threshold offset (dash line: $\Delta\mu < 0$, solid line: $\Delta\mu > 0$). (a) $\mu = 0.5$. (b) $\mu = 0.05$. (c) $\mu = 0.005$. (d) $\mu = 0.0005$

where B and τ are the bandwidth and integration time of the radiometer, respectively. η_Q is the efficiency of the 1B/2L correlator and could be calculated by [15]

$$\eta_Q = \frac{2\sqrt{\beta}}{\pi\sqrt{1 + 2\sum\limits_{q=1}^{\infty} R_2^2(q\tau_s)}} \tag{22}$$

where $\beta = F_s/2B$, F_s is the sampling frequency, $\tau_s = 1/F_s$, $R_2(\tau)$

Figure 2. Comparison between calibration methods. (a) Correlation error without calibration. (b) Correlation error calibrated by closed form approximation. (c) Correlation error calibrated by iteration method.

is the autocorrelation coefficient of the 2-level signal. For BHU-2D, $B = 160\,\mathrm{MHz}$, $\tau = 0.5\,\mathrm{s}$ and $F_s = 200\,\mathrm{MHz}$, therefore $\eta_Q = 0.470$ and $\sigma_\mu = 1.68 \times 10^{-4}$.

By calculating the boundary b of the threshold offset in BHU-2D, $|\Delta\mu|$ could be estimated and then the criterion could be employed to verify whether the closed form approximation is applicable.

The 1-bit quantizer in BHU-2D consists of an 8-bit ADC and a digital comparator. The threshold of the comparator, which is selected from one of the ADC output code, is always refreshed with the average of the signal. Thus, the threshold offset of the quantizer is no more than $\pm 0.5\,\mathrm{LSB}$ (least significant bit), i.e., $b \leq 0.5\,\mathrm{LSB}$. The maximum

input root-mean-square value of the ADC is about $255/6 = 42.5\,\mathrm{LSB}$ since the signal follows Gaussian distribution. Considering that the dynamic range of the radiometer is lower than $6\,\mathrm{dB}$, the minimum input root-mean-square value of the ADC is about $21.3\,\mathrm{LSB}$. Therefore b/σ is lower than 0.024. From Fig. 2(b), $|\Delta\mu| < 2 \times 10^{-7}$ could be concluded and Equation (20) could be met well. Therefore, the closed form calibration method is sufficient for BHU-2D.

## 3. DESCRIPTION OF THE CORRELATOR UNIT IN BHU-2D

Based on the principle and calibration method, the correlator unit of BHU-2D is designed and implemented. A simplified block diagram of the correlator unit is illustrated in Fig. 3. The input IF signals are digitized into 8-bit by 48 ADCs. With the 8-bit data, the power and averages of the signals are estimated. Then the averages are set as the threshold of the 1-bit quantizer. After quantizing into 1-bit, the signals are feed into 1B/2L correlator array to calculate Z^{raw}. Also a group of probability estimation elements are employed to computes $E[g_e(x, \Delta x)]$, which is used in the offset calibration procedure. In order to calibrate the quadrature error of the I/Q demodulator, the cross-correlations between the in-phase and quadrature channel of the receiver is also calculated in the correlator array except correlations corresponding to the baselines.
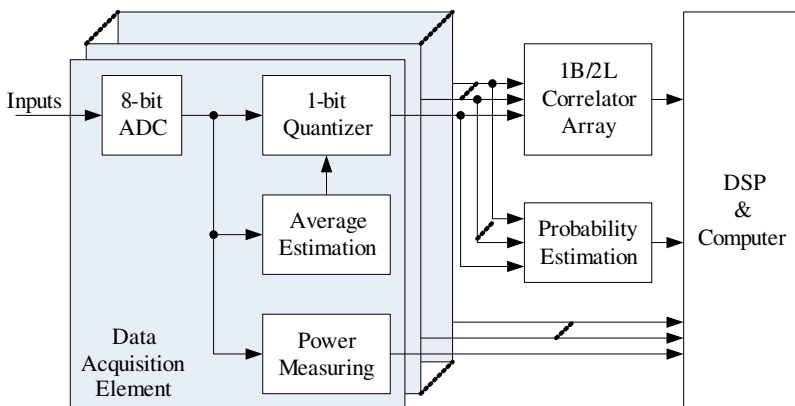
**Figure 3.** Block diagram of the correlator unit.
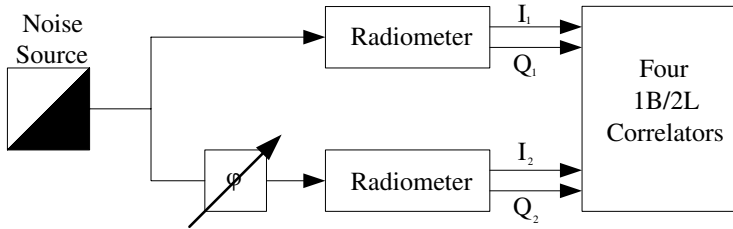
Figure 4. Diagram of the experiment setup for the correlation measurement.
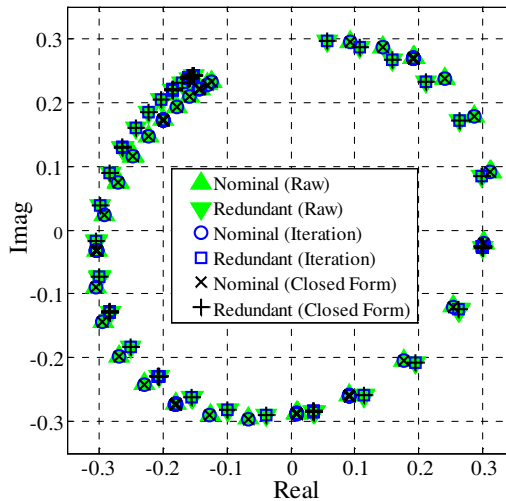
Figure 5. Comparison between iteration calibration and closed form calibration.

4. EXPERIMENT RESULT

Validation experiments for the correlator unit have been carried out, and results will be shown in this section. Fig. 4 illustrates the experiment setup. The noise source generates a noise signal and the excess noise ratio (ENR) is about 3 dB. The signal is fed into two Ka-band radiometers through a power splitter. In order to obtain different correlation coefficients, a phase-shifter is adopted to adjust the input phase of the second radiometer. Four 1B/2L correlators are used to calculate the complex cross-correlation coefficient between the output signals of the radiometers.
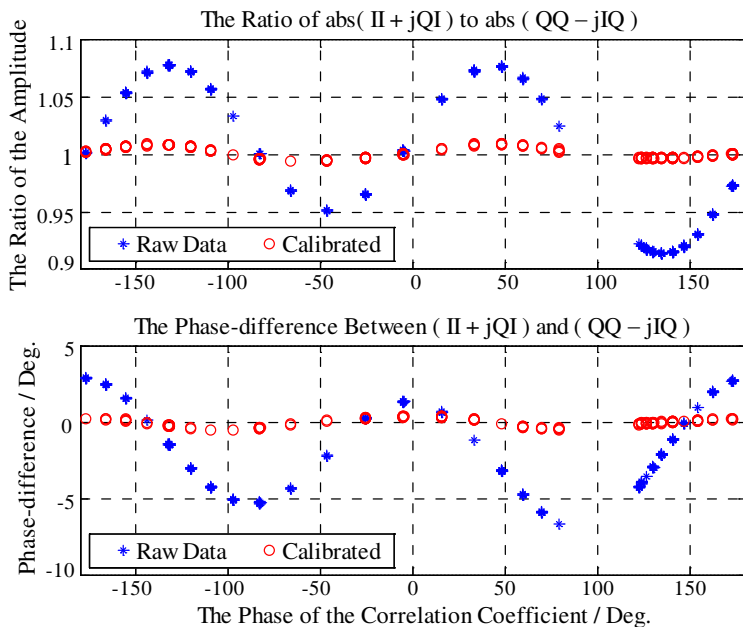
Figure 6. Comparison between nominal correlation coefficients (II + jQI) and redundant correlation coefficients (QQ − jIQ).

Considering the difficulty of obtaining the true value of the correlation coefficient within the required accuracy ($\Delta\mu \ll 1.68 \times 10^{-4}$), the results of iteration calibration method are employed to make a comparison with the results calculated by closed form approximation. The measured and calibrated complex correlation coefficients are shown in Fig. 5. The maximum deviation between raw data and calibrated data is 7.0×10^{-4}, while the maximum deviation between the two calibration methods is 4.8×10^{-8}. The result shows that closed form approximation is applicable in BHU-2D. After threshold offset calibration, the quadrature error and residual offset error are corrected. To validate the calibration methods, the comparison between the nominal correlation coefficients (II + jQI) and the redundant correlation coefficients (QQ − jIQ) are shown in Fig. 6. As is shown, the amplitude deviations between nominal and redundant correlation coefficients are reduced to ±1.1% and the phase-differences are reduced to ±0.6 degree after calibration procedures.

5. CONCLUSION

The design of the correlator unit for a two-dimensional synthetic aperture interferometric radiometer BHU-2D is presented in this paper. To deal with the throughput of $\sim$ 1000 correlators operating at 200 MHz, a FPGA based 1B/2L correlator array is employed. To calibrate the errors caused by the imperfection of the 1B/2L digitizer, the calibration methods are also presented. In order to reduce the processing time of the calibration procedure of the correlation coefficient, a closed form approximation used for correcting the threshold offset error of 1B/2L correlator is introduced and applied in BHU-2D. The approximation is of higher efficiency than the iteration calibration method adopted by MIRAS and HUT. Experiment results demonstrate that the performance of the approximation is sufficient for BHU-2D and other systems adopting 1B/2L correlators, although the accuracy of the method is lower than the iteration method. Our further effort will be focused on increasing the bandwidth of the correlator unit in low level quantization systems without high resolution ADCs in order to improve the radiometric sensitivity with reasonable volume, weight and power consumption.

REFERENCES

1. Le Vine, D. M., A. J. Griffis, C. T. Swift, and T. J. Jackson, "ESTAR: A synthetic aperture microwave radiometer for remote sensing applications," *Proc. IEEE*, Vol. 82, No. 12, 1787–1801, Dec. 1994.

2. Goodman, J. W., *Statistical Optics (Wiley Classics Library)*, 207–221, Wiley, New York, 2000.

3. Miao, J., "Microwave aperture synthetic radiometer and the passive millimeter wave imager of Beihang University," *Proc. ICMTCE*, 7, Beijing, China, May 22–25, 2001.

4. Van Vleck, J. H. and D. Middleton, "The spectrum of clipped noise," *Proc. IEEE*, Vol. 54, No. 1, 2–19, Jan. 1966.

5. Martin-Neira, M., I. Cabeza, C. Perez, M. A. Palacios, M. A. Guijarro, S. Ribo, I. Corbella, S. Blanch, F. Torres, N. Duffo, V. Gonzalez, S. Beraza, A. Camps, M. Vall-llossera, S. Tauriainen, J. Pihlflyckt, J. P. Gonzalez, and F. Martin-Porqueras, "AMIRAS — An airborne MIRAS demonstrator," *IEEE Trans. Geosci. Remote Sens.*, Vol. 46, No. 3, 705–716, Mar. 2008.

6. Rautiainen, K., H. Valmu, P. Jukkala, G. Moren, and M. Hal-

likainen, "Four-element prototype of the HUT interferometric radiometer," *Proc. IGARSS*, Vol. 1, 234–236, Hamburg, 1999.

7. Salmon, N. A., R. Macpherson, A. Harvey, P. Hall, S. Hayward, P. Wilkinson, and C. Taylor, "First video rate imagery from a 32-channel 22-GHz aperture synthesis passive millimetre wave imager," *Proc. SPIE*, Vol. 8188, 818805, Oct. 6, 2011.

8. Tanner, A. B., W. J. Wilson, P. P. Kangaslahti, B. H. Lambrigsten, S. J. Dinardo, J. R. Piepmeier, C. S. Ruf, S. Rogacki, S. M. Gross, and S. Musko, "Prototype development of a geostationary synthetic thinned aperture radiometer, GeoSTAR," *Proc. IGARSS*, Vol. 2, 1256–1259, Anchorage, AK, Sep. 20–24, 2004.

9. Ruf, C. S., "Digital correlators for synthetic aperture interferometric radiometry," *IEEE Trans. Geosci. Remote Sens.*, Vol. 33, No. 5, 1222–1229, Sep. 1995.

10. Camps, A., F. Torres, I. Corbella, J. Bara, and J. A. Lluch, "Threshold and timing errors of 1bit/2level digital correlators in Earth observation synthetic aperture radiometry," *Electron. Lett.*, Vol. 33, No. 9, 812–814, Apr. 1997.

11. Corbella, I., F. Torres, A. Camps, A. Colliander, M. Martín-Neira, S. Ribo, K. Rautiainen, N. Duffo, and M. Vall-llossera, "MIRAS end-to-end calibration: Application to SMOS L1 processor," *IEEE Trans. Geosci. Remote Sens.*, Vol. 43, No. 5, 1126–1134, May 2005.

12. Colliander, A., S. Tauriainen, T. I. Auer, J. Kainulainen, J. Uusitalo, M. Toikka, and M. T. Hallikainen, "MIRAS reference radiometer: a fully polarimetric noise injection radiometer," *IEEE Trans. Geosci. Remote Sens.*, Vol. 43, No. 5, 1135–1143, May 2005.

13. Camps, A., "Application of interferometric radiometry to earth observation," Ph.D. Dissertation, Ch. 4, Polytechnic University of Catalonia, Spain, 1996.

14. Camps, A., I. Corbella, J. Bara, and F. Torres, "Radiometric sensitivity computation in aperture synthesis interferometric radiometry," *IEEE Trans. Geosci. Remote Sens.*, Vol. 36, No. 2, 680–685, Mar. 1998.

15. Thompson, R., J. Moran, and G. Swenson, *Interferometry and Synthesis in Radio Astronomy*, 2nd Edition, 263, Wiley, New York, 2001.